A Fast Solver for Stokes Flow in 2D: [we need a better title]

Haiyang Wang, Nils Jan Fredrik Fryklund, Samuel Potter, Leslie Greengard

November 20, 2022

Abstract

In this paper, we exploit the *return to Poiseuille* phenomenon: a Stokes flow would quickly develop to the Poiseuille flow along a straight channel. This allows us to quickly solve the interior plane Stokes equation on a domain that is a union of *standard pieces*. Each standard piece is a pipe with inlets/outlets being long enough straight channels, such that when two standard pieces are connecting, where they connect is in middle of a long straight channel*, hence the flow at the connection would be close to Poiseuille flow within machine precision. Then, instead of solving stokes equation for the global domain, we can solve the Stokes equation for each standard pieces with boundary condition of Poiseuille velocity profile at inlets/outlets, and easily interface these local solutions to build a solution for the global domain.

Once the Stokes equation with boundary conditions of Poiseuille velocity profile is pre-solved on each standard piece, the standard pieces can be connected to form a complex domain of channel network. Interfacing the solutions of standard pieces would instantly give a high-order accurate solution of Stokes equation for the global domain. For example, in Figure 1, interfacing the local solutions took only 0.3 seconds, while directly solving on the global domain took 24 minutes.

1 Introduction

The *return to Poiseuille* phenomenon, or *Saint-Venant's principle* in the theory of plane elasticity, are well-established from the last century [3, 6, 7]. To be more specific, in a straight channel with laminar and incompressible incoming flow, the flow would quickly converge into a Poiseuille flow toward the outlet: the difference of the flow and the Poiseuille flow would decay at an exponential rate for Stokes flow. Therefore it is a good numerical hypothesis to assume that the flow is Poiseuille in middle of a lone straight channel, regardless of the incoming and outgoing flow.

For plane Stokes flow, the biharmonic equation formulation are well known and developed within theory of complex variable from the last century [8]. Various numerical schemes, such as boundary integral equation (BIE) and rational function approximation, have been developed accordingly [5, 12]. In this paper, we use the biharmonic BIE formulation for the plane Stokes equation from [5] to solve the Stokes equation on several standard pieces with Poiseuille boundary condition at inlets/outlets.

*The length of straight channel is greater than 7 times of the width, as indicated by Figure 4.

The main idea of this paper is to apply *Return to Poiseuille* as a high order accurate numerical hypothesis. It allows us to pre-solve a few standard pieces which have inlets and outlets being long enough straight channels, and are with boundary condition of Poiseuille velocity profile. Once the pre-solved, the *Return to Poiseuille* hypothesis allows us to interface solutions of Stokes flow on each standard pieces to get a solution for any complex channel networks that is a union of the standard pieces. Interfacing is by solving a system of linear equations, based on the constraints of zero-net-flux and continuity of pressure. This system of linear equations can be solved instantly and accurately.

This paper is organized as follows. In Section 2, we define the Stokes boundary value problem, the corresponding biharmonic boundary value problem, and then the integral equation of it. We also mention the analytic evidence and predicted exponential convergence rate for the *return to Poiseuille* in a semi-infinite straight channel. Then, we explain how to interface the local solutions of standard pieces by an simple example. In Section 3, we presents the Nyström discretization of the integral equation, which is solved iteratively by Generalized Minimal Residual Method (GMRES). The numerical experiments of connecting standard pieces and numerical evidence for *return to Poiseuille* hypothesis are contained in Section 4, followed by conclusions and possible further work in Section 5.

2 Mathematical Preliminaries

In this section, we briefly review the plane Stokes equation, its biharmonic form, and its biharmonic boundary integral equation. More detailed discussion can be found in [5]. Then, we will present an analytic estimate for the exponential decay rate of *return to Poiseuille* hypothesis [6], and explain how we have applied it as a numerical hypothesis: how to pre-solve each standard pieces and how to interface the pre-solved solutions for a domain of connected standard pieces.

2.1 Boundary Integral Equation

Stokes Boundary Value Problem. Recall that the plane Stokes equations are [8]:

$$\nu \Delta u = \frac{1}{\rho}\frac{\partial p}{\partial x}, \quad \nu \Delta v = \frac{1}{\rho}\frac{\partial p}{\partial y} \tag{1}$$

$$\frac{\partial u}{\partial x} + \frac{\partial v}{\partial y} = 0 \tag{2}$$

where u, v are components of velocity, p is the pressure, ρ and ν are the density and viscosity, which are constants. Another

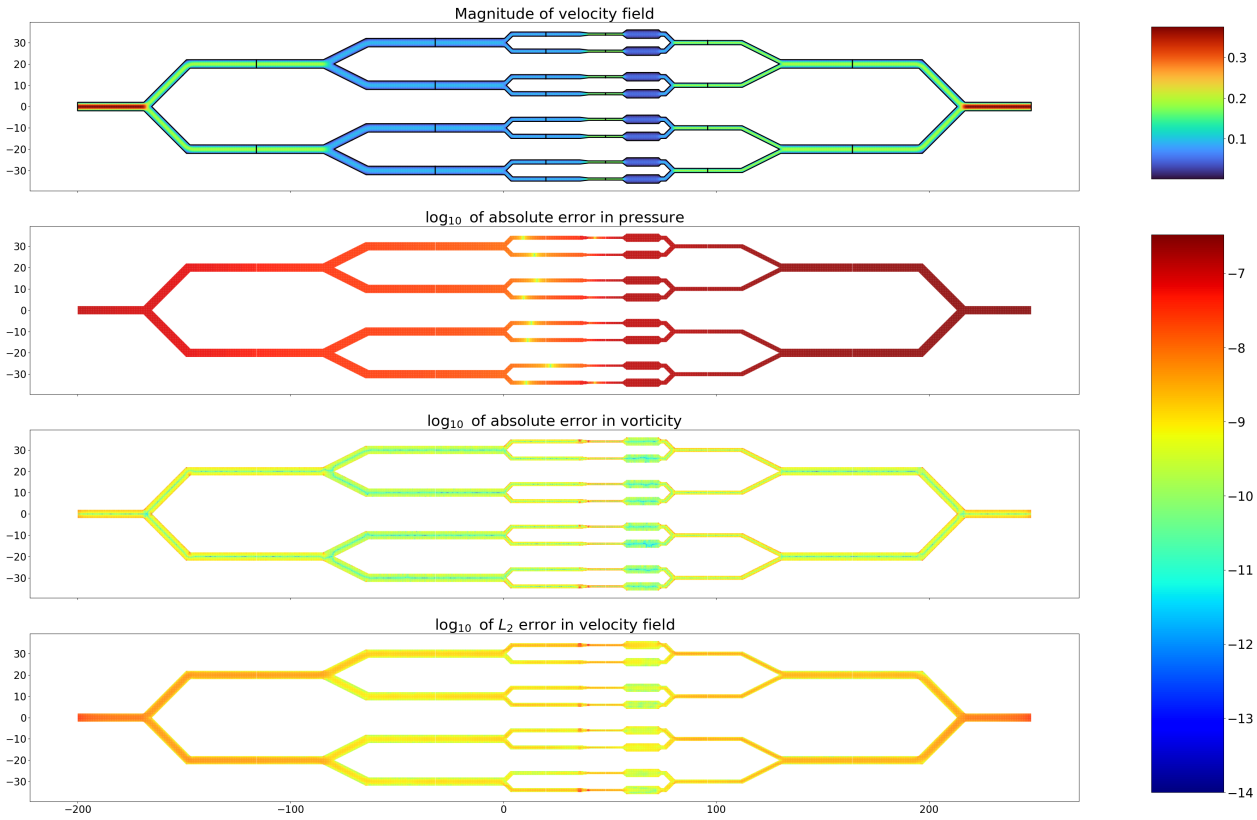

Figure 1: Solutions of the Stokes equation in a complex channel geometry as a union of 22 pieces of 7 kinds of standard pieces. The first sub-figure is a color-plot of magnitude of velocity field inside the domain, with colorbar on its right. The black lines in the first sub-figure marks the boundary of each standard piece. The other three sub-figures is color plot of absolute differences between the connected solution and the global solution in pressure, vorticity, and velocity field in the $\log_{10}$ scale, with colorbar on on the right. Each standard pieces are solved with required accuracy of 10^{-12} and the global domain is solved with required accuracy of 10^{-10}.

important physics quantity, vorticity, is defined as $\zeta = u_y - v_x$.

We are interested in Dirichlet boundary value problem (BVP) of Stokes equation on a bounded $(M+1)$-ply connected domain $D \subset \mathbb{R}^2$, with boundary $\partial D = \Gamma = \Gamma_0 \cup \Gamma_1 \cup \cdots \cup \Gamma_M$, where Γ_0 is the exterior boundary, and $\Gamma_1, \ldots, \Gamma_M$ are the interior boundaries. On the boundary Γ, the velocity is defined by given functions h_1, h_2:

$$u = h_2(t), \quad v = -h_1(t), \quad t \in \Gamma \tag{3}$$

For the specific purpose of this paper, the boundary velocity profile is zero everywhere except at the inlets/outlets of channels, where a Poiseuille velocity profile is specified.

Biharmonic Equation. (2) implies the existence of the stream function $W(x, y)$ such that [5]:

$$\frac{\partial W}{\partial x} = -v, \quad \frac{\partial W}{\partial y} = u \tag{4}$$

Following (1,2), it is easy to see that the stream function satisfies the biharmonic equation (5), and the Dirichlet BVP (3) can be understood as the following biharmonic BVP:

$$\Delta^2 W(x, y) = \Delta \zeta = 0, \qquad (x, y) \in D \tag{5}$$

$$\frac{\partial W}{\partial x} = h_1(t), \quad \frac{\partial W}{\partial y} = h_2(t), \qquad t \in \Gamma \tag{6}$$

Goursat's Formula. It has been long established that any plane biharmonic function $W(x, y)$ can be expressed by Goursat's formula [10]:

$$W(x, y) = \mathrm{Re}(\bar{z}\phi(z) + \chi(z)) \tag{7}$$

where the Goursat's functions ϕ, χ are analytic functions of complex variable $z = x + yi$. In the following, we will be identifying $(x, y) \in \mathbb{R}^2$ with $x + yi \in \mathbb{C}$.

Velocity, pressure, and vorticity can be conveniently expressed with the Goursat's functions. The Muskhelishvili's formula (8) expresses velocity field and another formula (9)

gives the pressure and vorticity [10]:

$$-v + ui = \frac{\partial W}{\partial x} + i\frac{\partial W}{\partial y} = \phi(z) + z\overline{\phi'(z)} + \overline{\psi(z)} \tag{8}$$

$$\zeta + \frac{i}{\nu}p = 4\phi'(z) \tag{9}$$

where $\psi = \chi'$.

The biharmonic boundary value problem (5,6), using the Muskhelishvili's formula (8), can be rewritten as

$$\phi(t) + t\overline{\phi'(t)} + \overline{\psi(t)} = h(t), \quad t \in \Gamma \tag{10}$$

where $h(t) = h_1(t) + ih_2(t)$, and t is understood as a complex variable.

Sherman-Lauricella Representation. The Sherman-Lauricella Representation proposes a specific form of the Goursat's functions [5]. And one can use this representation as an ansatz for BIE of the Biharmonic BVP (10). The Sherman-Lauricella representation is formulated as follows:

$$\phi(z) = \frac{1}{2\pi i}\int_\Gamma \frac{\omega(\xi)}{\xi - z}d\xi + \sum_{k=1}^{M} C_k \log(z - z_k) \tag{11}$$

$$\psi(z) = \frac{1}{2\pi i}\int_\Gamma \frac{\overline{\omega(\xi)}d\xi + \omega(\xi)\overline{d\xi}}{\xi - z} - \frac{1}{2\pi i}\int_\Gamma \frac{\overline{\xi}\omega(\xi)}{(\xi - z)^2}d\xi + \sum_{k=1}^{M}\left(\frac{b_k}{z - z_k} + \overline{C}_k \log(z - z_k) - C_k\frac{\overline{z}_k}{z - z_k}\right) \tag{12}$$

where ω is an unknown complex density on Γ to be solved, z_k are arbitrarily prescribed point inside the component curves Γ_k, and C_k, b_k are constants defined by:

$$C_k = \int_{\Gamma_k}\omega(\xi)|d\xi|, \quad b_k = 2\,\mathrm{Im}\int_{\Gamma_k}\overline{\omega(\xi)}d\xi \tag{13}$$

It is worthnoting that although ψ, ϕ might be multiple-valued, the velocity, pressure, and vorticity are single-valued functions of z.

Boundary Integral Equation. Plugging the Sherman-Lauricella representation (11,12) into equation (10), and letting a point z in the interior of D approach to a point on the boundary $t \in \Gamma$ in (10), the classical formulae for the limiting values of Cauchy-type integral gives us the following integral equation for ω [9, 5]:

$$\begin{aligned}\omega(t) &+ \frac{1}{2\pi i}\int_\Gamma \omega(\xi)d\ln\frac{\xi - t}{\overline{\xi - t}} - \frac{1}{2\pi i}\int_\Gamma \overline{\omega(\xi)}d\frac{\xi - t}{\overline{\xi - t}} \\ &+ \sum_{k=1}^{M}\left(\frac{\overline{b}_k}{\overline{t - z_k}} + 2C_k\log|t - z_k| + \overline{C_k}\frac{t - z_k}{\overline{t - z_k}}\right) \\ &+ \frac{\overline{b}_0}{\overline{t - z^*}} \\ &= h(t)\end{aligned} \tag{14}$$

the extra term $\frac{\overline{b}_0}{\overline{t-z^*}}$ vanishes when the zero-net-flux condition $\mathrm{Re}\int_\Gamma \bar{h}(t)dt = 0$ is satisfied, hence will be omitted in the Nyström discretization of (14) later. The invertibility of this integral equation is similar to the standard proof of invertibility for elasticity problems [10, 5], and are omitted.

2.2 Return to Poiseuille

In this section, we will first show the analytic estimate for the *return to Poiseuille* phenomenon, which is based on eigenfunction analysis on a domain of a semi-infinite straight channel from the theory of plane elasticity [6]. Then, we explain how to apply the *return to Poiseuille* hypothesis, and how to interface the solutions on standard pieces.

Analytic Estimate for Return to Poiseuille. On the domain of a semi-infinite straight channel $D_L = \{(x, y) \mid x \geq 0, |y| \leq L\}$, with the boundaries

$$\begin{aligned}\Gamma_L &= \Gamma_L^1 \cup \Gamma_L^2 \cup \Gamma_L^3 \\ &= \{(0, y)||y| \leq L\} \cup \{(x, L)|x \geq 0\} \cup \{(x, -L) \mid x \geq 0\}\end{aligned} \tag{15}$$

where Γ_L^2, Γ_L^3 are walls with the non-slippery boundary conditions, and Γ_L^1 is the inlet with boundary condition of an incoming laminar incompressible flow. *Return to Poiseuille* means that regardless of the boundary velocity profile on Γ_L^1, the flow's profile at $x = l$ will converge Poiseuille flow of same flux as $l \to \infty$.

Without lost of generality, assume there is zero net flux across Γ_L^1. Then, *return to Poiseuille* is equivalent to return to the zero flow, i.e. the flows velocity profile at the vertical cross-section $x = l$ would converge to zero at an exponential decay rate as $l \to \infty$. The BVP can be formulated as the following:

$$\frac{\partial W(x, y)}{\partial y} = W(x, y) = 0, \qquad (x, y) \in \Gamma_L^2 \cup \Gamma_L^3 \tag{16}$$

$$\frac{\partial W(0, y)}{\partial x} = f(y), \ \frac{\partial W(0, y)}{\partial y} = g(y), \quad (0, y) \in \Gamma_L^1 \tag{17}$$

where f, g are smooth enough functions satisfying $f(\pm L) = g(\pm L) = \int_{-L}^{L} g(y)dy = 0$, so that the net-flux is zero and the boundary condition is continuous.

This biharmonic BVP is identical to the self-equilibrated traction BVP in the theory of elasticity studied in [6, 7, 3]. When f''', g''' exist and are of bounded variation, this problem has a unique solution spanned by the Papkovich-Fadle eigenfunctions [6]. The absolute value of first eigenfunction is dominated by $e^{-xk/2L}$, where

$$k \simeq 4.2^\dagger$$

This gives the decay rate of return to Poiseuille hypothesis, which agrees with our numerical experiment in Figure 4.

Return to Poiseuille as a Numerical Hypothesis. Given the analytic estimate above, it is easy to see that in a straight channel with length greater than 8 times of the channel width, we can expect the flow to be Poiseuille with 14th digits of accuracy at the outlet regardless of the velocity profile on the inlet. Therefore, it is appropriate to require the inlets/outlets of the standard pieces to be such straight channels, and assign the Poiseuille boundary conditions on the inlets/outlets.

†This is the smallest positive real parts of the roots of the transcendental equation $\sin^2\lambda - \lambda^2 = 0$.

Figure 1 is a numerical example where the interfaced solution is compared with a global solution, and high order accuracy is achieved in both pressure, velocity, and vorticity. It is worth-noting that no significant numerical error is observed at where the standard pieces are connected.

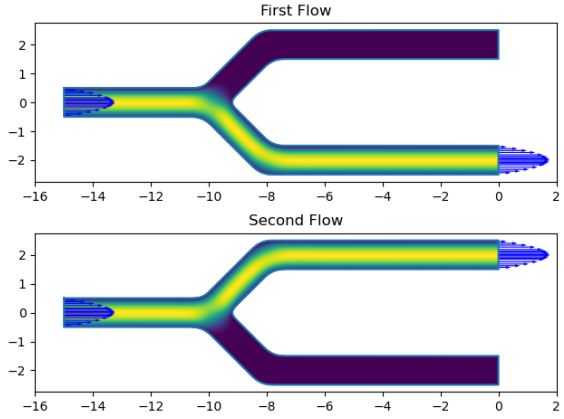

Figure 2: The 2 generating flows for a Y-shaped standard piece: the color inside the domain denotes the magnitude of the velocity of the flow, the blue arrow denotes the boundary condition of unit-flux Poiseuille velocity profile at the inlets/outlets.

Interface the Solutions on Standard Pieces. For a standard piece with a total number of m inlets/outlets, the boundary conditions of our interest, Poiseuille at the inlets/outlets and non-slippery elsewhere, can be simply characterized by the flux of the Poiseuille flow at each inlet/outlet. The fluxes need to sum to zero, so the boundary conditions is a $m-1$ dimensional space. As the Stokes equation is linear, this means we only need to solve for $m-1$ flows on the standard piece, and superimpose these flows would give us any flow in the standard piece with boundary condition of Poiseuille at inlets/outlet and non-slippery elsewhere. For example, in Figure 2, a standard piece of Y shaped standard pieces, with a total number of 3 inlets/outlets, are pre-solved with 2 generating flows.

With the the generating flows pre-solved for each standard piece, interfacing these flows is reduce to finding appropriate fluxes of the generating flows of the standard pieces such that:

1. The fluxes matches at where the point of connection.
2. The pressure is a continuous function across the domain.

The second condition is needed only when the domain of connected standard pieces have cycles, i.e. the domain is not simply connected.

To demonstrate how these two conditions are turned into a linear system of equations for interfacing local solutions, let us consider the specific example in Figure 3a, where the global domain is two connected Y-shaped standard pieces. The global domain is given with flux $f_{-1} = -1$ (incoming) at the left inlet and flux $f_{-2} = 1$ (outgoing) at the right outlet. Each standard piece has two fluxes of generating flows need to be solved for, so there are total number of 4 fluxes f_0, f_1, f_2, f_3 needs to be solved for.

This problem can be abstracted into a graph theory problem as in Figure 3b, where the the nodes V_0, V_1, V_2, V_3 denotes the interfaces among the standard pieces and global boundary conditions of fluxes, The edge $E_{0,1}, E_{0,2}, E_{31}, E_{32}$ represents the generating flows with the fluxes f_0, f_1, f_2, f_3 to be solved for. The fluxes f_{-1}, f_{-2} are given on superficial edges representing the boundary fluxes of the global domain.

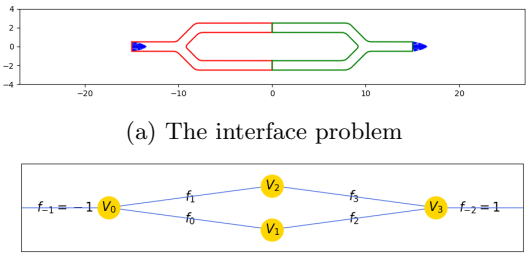

(a) The interface problem

(b) The abstract network for the interface problem

Figure 3: A simple interface problem with 2 Y-shaped standard pieces.

The interface condition 1 of agreeing fluxes at the interfaces, in this graph theory setting, can be understood as the following: at each node, its adjacent edges have fluxes sum to zero. Requiring this to be true at all nodes gives us the following linear system of equations:

$$\begin{pmatrix} 1 & 1 & 0 & 0 \\ 1 & 0 & 1 & 0 \\ 0 & 1 & 0 & 1 \\ 0 & 0 & 1 & 1 \end{pmatrix} \begin{pmatrix} f_0 \\ f_1 \\ f_2 \\ f_3 \end{pmatrix} = \begin{pmatrix} -f_{-1} \\ 0 \\ 0 \\ -f_{-2} \end{pmatrix} = \begin{pmatrix} 1 \\ 0 \\ 0 \\ -1 \end{pmatrix} \tag{18}$$

This matrix has rank 1 deficiency. This rank deficiency is due to there is 1 cycle in the graph. This rank deficiency can be resolved by the continuity of pressure condition 2.

Continuity of pressure, or single valued-ness of pressure, can be understood as that the pressure p_i at each node V_i is a well-defined single-value function. This condition would be automatically satisfied by the flux condition 1 if the global domain is simply connected. However, for a domain with cycles, such as the cycle (V_0, V_1, V_3, V_2) in Figure 3b, single-valued-ness of pressure can be understood as the pressure drops along the cycle would sum to zero. Therefore, we can gain a new equation:

$$p_{10} + p_{31} + p_{23} + p_{02} = 0 \tag{19}$$

where p_{ij} is the pressure drop from node V_j to node V_i. The pressure drops p_{ij} depends linearly on the fluxes of generating flows of the standard pieces, For this case, p_{10}, p_{02} are linear functions of f_0, f_1, and p_{31}, p_{23} are linear functions of f_2, f_3. These linear functions can be computed in the pre-solving process, and for this example, they are

$$\begin{pmatrix} p_{10} \\ p_{02} \end{pmatrix} = \begin{pmatrix} -46.02 & -14.78 \\ 14.78 & 46.02 \end{pmatrix} \begin{pmatrix} f_0 \\ f_1 \end{pmatrix} \tag{20}$$

$$\begin{pmatrix} p_{31} \\ p_{23} \end{pmatrix} = \begin{pmatrix} 46.02 & 14.78 \\ -14.78 & -46.02 \end{pmatrix} \begin{pmatrix} f_2 \\ f_3 \end{pmatrix} \tag{21}$$

Combining equations (19), (20) and (21), we have:

$$(46.02 - 14.78)(-f_0 + f_1 + f_2 - f_3) = 0 \tag{22}$$

which completes (18) to a full rank linear system of equations and with the solutions $(f_0, f_1, f_2, f_3) = (0.5, 0.5, -0.5, -0.5)$.

The process of interfacing local solutions in the example of Figure 3 can be generalized into a algorithm for interfacing of any connected standard pieces. The key idea of the algorithm is rather simple: generating the appropriate linear equations of matching fluxes and matching pressure drops, and then solving for fluxes of generating flows. However, it involves troublesome bookkeeping of the correspondence between the graph theory problem and the generating fluxes and pressure-drops of each standard pieces, so the detailed and complete description of the algorithm is omitted here. One can find source code for this algorithm at `https://github.com/WangHaiYang874/stokes2d`.

Numerical Stability of Interface Algorithm The numerical stability of the connecting algorithm can be analyzed as follows. The condition of matching fluxed 1 is translated to the linear equation (18), which contains only $1, 0$ and therefore no inaccuracy is introduced. The only inaccuracy is introduced by computing of the matrices in (20) and (21) in the pre-solving process. Each entries of the matrices of pressure drops can be computed with required accuracy of $\epsilon = 10^{-12}$, Therefore ...

3 Description of Numerical Methods

In this section, we will first present Nyström discretization of boundary integral equation (14). And we will briefly explain the smoothing of the geometry and accurate near boundary evaluation of layer potential.

3.1 Boundary Integral Equation

The boundary curve Γ_k is given by the parametrization $\Gamma_k = \{t^k(a) : a \in [A_k, A_{k+1}]\}$, and discretized into N_k points $t_i^k = t^k(a_i^k)$. Associate to each point t_j^k are the unknown complex density ω_j^k, the derivative $d_j^k = t^{k\prime}(a_j^k)$, and the quadrature weight w_j^k. In total, we have $N = \sum_{k=0}^{M} N_k$ points. The Nyström discretization of BIE (14) is:

$$\omega_j^k + \sum_{m=0}^{M}\sum_{n=1}^{N_k} K_1(t_j^k, t_n^m)\omega_j^k + \sum_{m=0}^{M}\sum_{n=1}^{N_k} K_2(t_j^k, t_n^m)\overline{\omega_j^k} = h_j^k \tag{23}$$

where $h_j^k = h(t_j^k)$ and the kernels K_1, K_2 are given by

$$K_1(t_j^k, t_n^m) = \frac{w_n^m}{\pi}\,\mathrm{Im}\left(\frac{d_n^m}{t_n^m - t_j^k}\right) + K_1^s(t_j^k, t_n^m) \tag{24}$$

$$K_2(t_j^k, t_n^m) = \frac{w_n^m}{\pi}\frac{\mathrm{Im}((t_n^m - t_j^k)\overline{d_n^m})}{(\overline{t_n^m - t_j^k})^2} + K_2^s(t_j^k, t_n^m) \tag{25}$$

with K_1^s, K_2^s representing the singular sources are:

$$K_1^s(t_j^k, t_n^m) = \delta_m w_n^m \left(\frac{i\overline{d_n^m}}{\overline{t_j^k - z_m}} + 2\log|t_j^k - z_m|\right) \tag{26}$$

$$K_2^s(t_j^k, t_n^m) = \delta_m w_n^m \frac{t_j^k - z_m - id_n^m}{\overline{t_j^k - z_m}} \tag{27}$$

where $\delta_m = 1$ excepts for $\delta_0 = 0$. In the limiting case of $t_j^k = t_n^m$, the value of K_1, K_2 are:

$$K_1(t_j^k, t_j^k) = \frac{w_j^k \kappa_j^k |d_j^k|}{2\pi} + K_1^s(t_j^k, t_j^k) \tag{28}$$

$$K_2(t_j^k, t_j^k) = -\frac{w_j^k \kappa_j^k (d_j^k)^2}{2\pi|d_j^k|} + K_2^s(t_j^k, t_j^k) \tag{29}$$

where κ_j^k is the signed curvature at the point t_j^k.

The Nyström discretizetion (23) can be written more compactly as the following matrix equation:

$$\omega + K_1\omega + K_2\overline{\omega} = h \tag{30}$$

This equation is separated into real and imaginary parts, and iteratively solved by the GMRES [11]. For each GMRES iteration, evaluating the left hand side of (30) is required, and evaluating by a dense matrix-vector product would require space and time complexity of $O(N^2)$. Too expensive when N is large. Therefore, we used a biharmonic fmm provided by the Flatiron Institute instead, which would only have time and space complexity of $O(N)$ [1].

The matrix equation (30) obeys the zero-net-flux condition, therefore only has solution when $\mathrm{Re}\int_\Gamma \overline{h(t)}dt = 0$. This also means that (30) has rank deficiency, which might cause GMRES converging slowly. This issue can be avoided by adding a double layer term

Evaluation of the layer potentials near boundary is done as in [13].

3.2 Geometry of the Boundary

The key to spectral convergence of GMRES is to have smooth boundary, or for piecewise smooth boundary, one can use special treatment as in [13] to ensure the spectral convergence is preserved. Here for this paper, we focused on smooth geometry. We adopted the ideas from [4, 2] to smooth the corners of the boundary by convolution, and added superficial caps at the inlets and outlets. [insert a figure here]. The geometry is adaptively discretized into Gauss-Legendre panels, as described in [13].

4 Numerical Results and Discussion

4.1 Numerical evidence of return to poiseuille

The numerical evidence for return to Poiseuille phenomenon is demonstrated on a straight pipe of width 1 and length 8 as in Figure 4. On the left boundary, a smooth velocity profile is imposed. This velocity profile is an arbitrarily picked smooth function that satisfies the requirement of equation (17). On the rest of the curve, non-slippery condition is imposed.

Figure 4a shows that the rate of returning to the zero flow is agreed with the predicted rate from Section 2.2 up to 14th digits of accuracy. Figure 4b is a color plot where the color indicates the $\log_{10}$ of absolute value of the velocity, pressure, and vorticity.

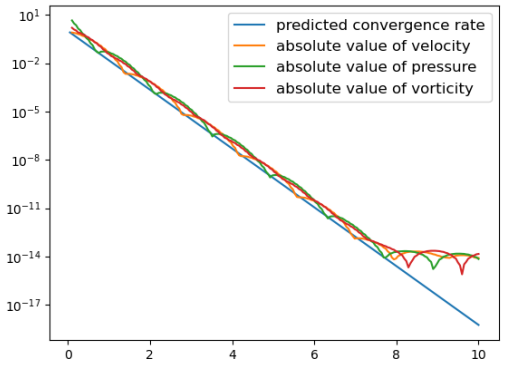

(a) Numerical Convergence rate of return to Poiseuille flow in a straight channel

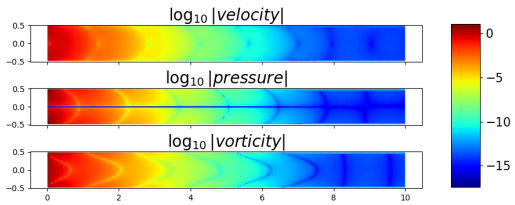

(b) $\log_{10}$ of the absolute value of the velocity, vorticity, and pressure within the straight channel.

Figure 4: Numerical exponential rate for return to Poiseuille flow. This is solution of Stokes BVP on a straight channel of length 10 and width 1, with non-slippery boundary condition on the top and bottom walls, an incoming flow (smooth and randomly generated) of zero-net-flux on the left inlet, and no outgoing flow on the right outlet. (a) The semilogy of magnitude of velocity, pressure, and vorticity along each vertical cross section along the channel. (b) The color plot of the magnitude of velocity, pressure, and vorticity in $\log_{10}$ scale in the straight channel.

4.2 a complicated network of pipes to show the power of this method

5 Conclusions

6 Acknowledgements

We thank Charles S. Peskin and Manas Rachh for many useful discussions pretaining to this work. We thank Manas Rachh and Libin Lu for providing support for the Flatiron Institute's FMM2D library [1].

6.1 summarize what I've done

6.2 outlook. What other work might be followed?

References

[1] Flatironinstitute/fmm2d.

[2] Joar Bagge and Anna-Karin Tornberg. Highly accurate special quadrature methods for Stokesian particle suspensions in confined geometries. 93(7):2175–2224.

[3] Horgan Co. Recent developments concerning Saint-Venant's principle,". In *In Advances in Applied Mechanics, TY Wu and JW Hutchinson (Eds), Vol 23,*, pages 179–269. Academic Press,.

[4] Charles L. Epstein and Michael O'Neil. Smoothed corners and scattered waves.

[5] Leslie Greengard, Mary Catherine Kropinski, and Anita Mayo. Integral Equation Methods for Stokes Flow and Isotropic Elasticity in the Plane. 125(2):403–414.

[6] R. D. Gregory. The traction boundary value problem for the elastostatic semi-infinite strip; existence of solution, and completeness of the Papkovich-Fadle eigenfunctions. 10(3):295–327.

[7] C. O. HORGAN. DECAY ESTIMATES FOR THE BIHARMONIC EQUATION WITH APPLICATIONS TO SAINT-VENANT PRINCIPLES IN PLANE ELASTICITY AND STOKES FLOWS. 47(1):147–157.

[8] O. A. Ladyzhenskaya, Richard A. Silverman, Jacob T. Schwartz, and Jacques E. Romain. *The Mathematical Theory of Viscous Incompressible Flow*. 17(2):57–58.

[9] Nikolaj I. Muschelišvili and Nikolaj I. Muschelišvili. *Singular Integral Equations: Boundary Problems of Function Theory and Their Application to Mathematical Physics*. Wolters-Noordhoff Publishing, softcover reprint of the original 1st ed. 1958 edition.

[10] N. I. Muskhelishvili. *Some Basic Problems of the Mathematical Theory of Elasticity*. Springer Netherlands.

[11] Youcef Saad and Martin H. Schultz. GMRES: A Generalized Minimal Residual Algorithm for Solving Nonsymmetric Linear Systems. 7(3):856–869.

[12] Lloyd N. Trefethen. *Approximation Theory and Approximation Practice, Extended Edition*. Society for Industrial and Applied Mathematics.

[13] Bowei Wu, Hai Zhu, Alex Barnett, and Shravan Veerapaneni. Solution of Stokes flow in complex nonsmooth 2D geometries via a linear-scaling high-order adaptive integral equation scheme. 410:109361.